Thermally-Electrically Tunable Graphene-Based Guided-Mode Resonant Perfect Absorber

Ze-Tao Huang, Hao-Yi Jiang, Zi-Ye Wang, Ye-Ming Qing, and Bing-Xiang Li

***Abstract*— We propose a thermally-electrically tunable perfect absorber based on amorphous silicon (a-Si) and graphene. Numerical results reveal that a perfect absorption with narrow bandwidth can be induced owing to the guided-mode resonance. The thermal tuning of resonant wavelength, realized via the Joule heating, characters a high tuning efficiency and a linear controllability. The linear and thermal tunability is attributed to the linear relationship between refractive index of a-Si and temperature. Moreover, by adjusting the applied gate voltage, the chemical potential of graphene can be electrically modified, leading to a change of optical absorption and enabling a rapid switching of perfect-absorption and perfect-reflection. It is remarkable that the proposed absorber features a simple structure, perfect absorption, and efficient thermal-electric tunability, manifesting tremendous potential applications in modulator, optical switching, selective filter, etc.**

***Index Terms*— Thermal-electric tunability, graphene, high-quality factor, guided-mode resonance, perfect absorber.**

I. Introduction

GRAPHENE, a newly found two-dimensional material with a single layer of carbon atoms, has been intensively investigated due to its outstanding optoelectronic properties. [1] Various graphene-based optoelectronic devices have been proposed such as optical modulators, [2] filters, [3], [4], [5] absorbers [6], and polarizers, [7], [8] etc., thanks to the fast carrier mobility, wide operating frequency range, and flexible tunability of graphene. Of great interest is that the plasmonic response of graphene significantly enhances the optical absorption in the infrared to terahertz (THz) ranges through strong light-graphene interaction. [9] In contrast, the plasmonic resonance is no longer sustained in the visible to near-infrared regions (NIR) since graphene behaves mostly like an absorptive dielectric, which extremely hinders its relevant applications in this wavelength region. Over the past decades, a variety of researches have been reported to promote absorption in this region. Piper et al. numerically demonstrated total absorption in graphene via critical coupling with guided-mode resonance and photonic band gap. [10] Hu et al. proposed a subwavelength grating with a three-period-silica/silicon structure covered by graphene strips, which is able to succeed a total absorption. [11] Furthermore, much progress has been made to design thermally adjustable devices with flexible tunability via temperature phase change materials like Vanadium dioxide (VO_2) and $Ge_2Sb_2Te_5$ (GST). It has been confirmed that these materials experience a great variation of optical properties during the phase change process. [12], [13] A thermally tunable absorber, reported by Wen et al., can induce two resonant absorption peaks by applying a complete VO_2 film. [14] A remarkable work proposed by Liu et al. demonstrated a broadband tunable absorber based on VO_2 with a tunable absorption in range of 5% to 100% by an external thermal excitation. [15] However, the devices based on VO_2 or GST challenge not only a wide bandwidth but also a high phase change temperature (around 68 °C), [16] which should be obstacles to select the target wavelength or tune optic properties.

To address these issues, a guided-mode resonance (GMR) type thermally-electrically tunable optical absorber is proposed in NIR based on a-Si and graphene. Concretely speaking, perfect absorption can be induced owing to GMR by our purposeful design. In the system, a variation of refractive index of a-Si can be carried out by modulating temperature, resulting in a linear and nondestructive drift of the absorption peak. Additionally, a switching of perfect-absorption state and perfect-reflection state can be realized by electrically manipulating the chemical potential of graphene. The finite element method (FEM) is employed to obtain the optical response of the system. The reported graphene-based absorber characterizes simple structure, perfect absorption, high-quality factor, and flexible thermal-electric adjustability, which may hold potential in optoelectronic devices fabrication in NIR.

II. Structure and Theory

The schematic of the proposed structure is shown in Fig. 1(a). [4], [6] The graphene monolayer is sandwiched between the subwavelength diffraction grating layer and the dielectric slab. A lossless metallic mirror is placed on the bottom of the structure to block all transmission. As for a-Si, its refractive index n has a linear relationship with temperature T: $n = n_0 + \alpha(T - T_0)$, where n_0 is set to 3.42 at the room temperature $T_0 = 20\,^{\circ}\mathrm{C}$, α is the thermal-optic coefficient with a value of 3.25×10^{-4} /°C. [17] The structural parameters of

Manuscript received 17 November 2022; revised 6 December 2022; accepted 8 December 2022. Date of publication 12 December 2022; date of current version 3 January 2023. This work was supported in part by the National Key Research and Development Program of China under Grant 2022YFA1405000, in part by the Natural Science Foundation of Jiangsu Province under Grant BK20222004, in part by the National Natural Science Foundation of China under Grant RK106LH21001, and in part by the Natural Science Research Start-up Foundation of Recruiting Talents of Nanjing University of Posts and Telecommunications under Grant NY222080. *(Corresponding authors: Ye-Ming Qing; Bing-Xiang Li.)*

The authors are with the College of Electronic and Optical Engineering and the College of Flexible Electronics (Future Technology), Nanjing University of Posts and Telecommunications, Nanjing 210023, China (e-mail: ymqing@njupt.edu.cn; bxli@njupt.edu.cn).

Color versions of one or more figures in this letter are available at https://doi.org/10.1109/LPT.2022.3228853.

Digital Object Identifier 10.1109/LPT.2022.3228853

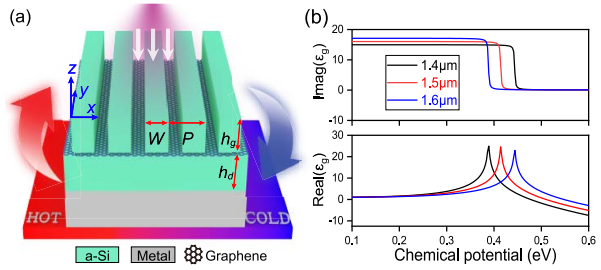

Fig. 1. (a) Schematic diagram of the absorber. (b) The permittivity of graphene monolayer depends on chemical potential at different wavelengths.

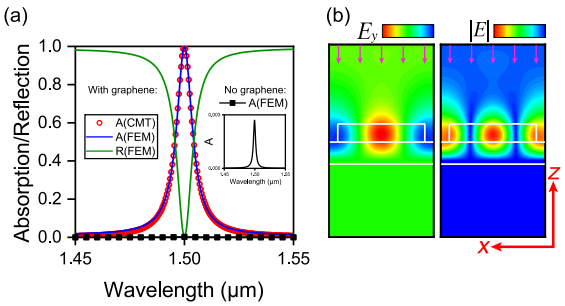

Fig. 2. (a) Absorption (A) and reflection (R) spectra from CMT fitted values and FEM simulation results. (b) Distribution map of E_y and $|E|$ for GMR mode at 1500 nm.

the absorber are: $P = 669$ nm, $W = 578$ nm, $h_g = 138.2$ nm, $h_d = 116.5$ nm, respectively. The designed center wavelength λ_c is set to 1500 nm. The graphene monolayer is ideally assumed as an ultrathin dielectric film with a thickness of $t = 0.34$ nm. The permittivity ε_g of graphene can be modeled as $\varepsilon_g = 1 + i\sigma_g/(\omega\varepsilon_0 t)$, where σ_g is graphene surface conductivity, ω is angular frequency of the incident wave, and ε_0 is vacuum permittivity, respectively. [18] The conductivity σ_g of the graphene can be written from the Kubo formula: [19]

$$\sigma_g = i\frac{e^2 k_B T}{\pi\hbar^2\left(\omega + i\tau^{-1}\right)}\left[\frac{\mu_c}{k_B T} + 2\ln\left(\exp\left(-\frac{\mu_c}{k_B T}\right) + 1\right)\right] + i\frac{e^2}{4\pi\hbar}\ln\left[\frac{2|\mu_c| - \hbar\left(\omega + i\tau^{-1}\right)}{2|\mu_c| + \hbar\left(\omega + i\tau^{-1}\right)}\right], \quad (1)$$

where $i = \sqrt{-1}$. e, k_B, T, $\hbar$, μ_c are electron charge, Boltzmann constant, temperature, reduced Planck's constant, and chemical potential, respectively. The chemical potential μ_c is set to 0.3 eV in our model. All the other graphene parameters are set the same as those in [6]. Intriguingly, a variation of ε_g can be realized by varying μ_c, as shown in Fig. 1(b).

According to the coupled mode theory (CMT), the absorptivity of the system can be written as: [20]

$$A = 1 - |r|^2 = \frac{4\delta\gamma}{(\omega - \omega_0)^2 + (\delta + \gamma)^2}, \quad (2)$$

where δ, γ, ω_0 represent the intrinsic loss of guided resonance, external leakage rate of the structure and resonant angular frequency. The perfect absorption should generate at resonant angular frequency ω_0 when $\delta = \gamma$. Meanwhile, we introduce an electromagnetic model for a multilayer planar structure based on the classical slab waveguide theory (CSWT) to further analyze the physical mechanism. [21] One can calculate the resonant wavelength by CSWT in terms of structural parameters, material properties, etc. As a result, CSWT can be another theoretical verification of the simulation. In our work, CSWT is utilized to obtain the resonant wavelength of the specifical system, and absorptivity of the corresponding incident wavelength can be estimated by CMT. Intriguingly, the similar mechanism, silicon hot-carrier induced electroluminescence with the MOS-like resonance, can be reasonably associated according to formulas 1 and 2, which may be potentially useful for optoelectronic applications. [22]

III. Results and Discussion

Figure 2 demonstrates the simulation results of our proposed absorber with TE plane wave probing vertically. As shown in Fig. 2(a) that the absorptivity reaches 99.99% at center wavelength $\lambda_0 = 1500$ nm. (Other center wavelengths within NIR are acceptable.) A great agreement between FEM and CMT can be observed in the figure, illustrating that CMT provides a relevant interpretation for the single port system. The absorption of the no-graphene structure is also shown in the figure so as to prove the enhancement caused by graphene. Furthermore, the full width at half maximum (FWHM) in our absorber is only $\Delta\lambda = 8.6$ nm and such a narrow bandwidth implies an excellent capability for spectral selection absorption. Interestingly, the bandwidth of the spectrum can be optimized by means of modifying incident wavelength and angle. To better describe the absorption performance of the system, we introduce a quality factor $Q_0 = \lambda_0/\Delta\lambda$. In our system, a high agreement between $Q_0 = 174.42$ and $Q_{CMT} = 174.53$ greatly manifests a practical feasibility of CMT in our system. Meanwhile, the sensitivity should be of great interest for optoelectronic devices, and therefore we introduce the figure of merit (FoM): $FoM = S/\Delta\lambda$, $S = \Delta\lambda_0/\Delta n$, where $\Delta\lambda_0$ is the spectral shift resulted from the refractive index change Δn. In our model, $\Delta n = 0.01$ leads to $\Delta\lambda_0 = 4.2$ nm and the measured FWHM is $\Delta\lambda = 8.6$ nm. The corresponding $FoM = 48.84$ of our absorber is somewhat superior to most nanostructures (about 40). The distributions of electric field amplitude E_y and electric field intensity $|E|$ in the configuration are depicted in Fig. 2(b) to provide an intuitionistic understanding of the mechanism of the enhanced light absorption effect. According to the guided-mode resonance theory, a proper periodicity of the diffraction grating enables phase-matching coupling between guided-mode and free-space radiation, arousing a typical standing wave in the structure and exciting a GMR mode. As shown in Fig. 2(b), several nodes are concentrated near the grating sheet, which allows lossy material graphene consume more electromagnetic energy. Consequently, the absorption of the graphene extremely increases, leading to a perfect absorption of the system.

To further expose the potential mechanism, GMR under different modes is investigated. It is demonstrated in Fig. 3(a) that three local absorption peaks are generated in the spectrum, indicating that three different GMR modes can be excited

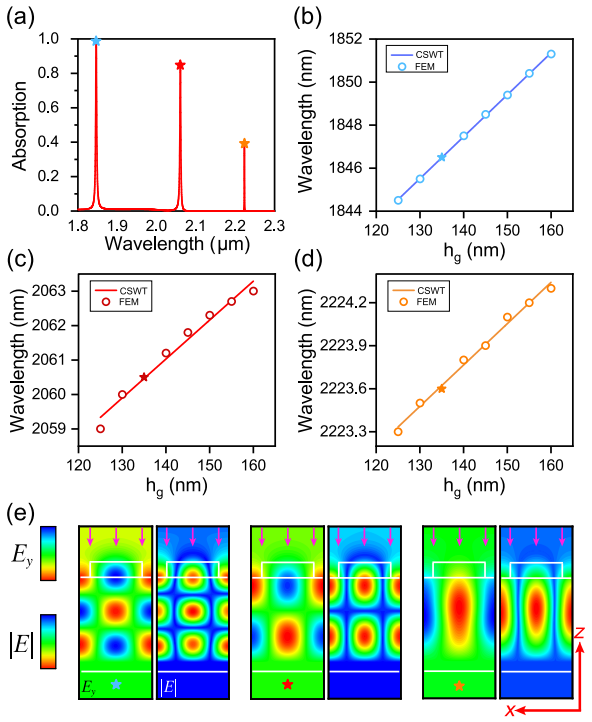

Fig. 3. (a) Absorption spectra with different incident wavelengths. The corresponding distribution map of E_y and $|E|$ of different peaks marked with different colors are shown in (e). The linear dependence of resonant wavelength on h_g of (b) third-order, (c) second-order, and (d) first-order are represented, respectively.

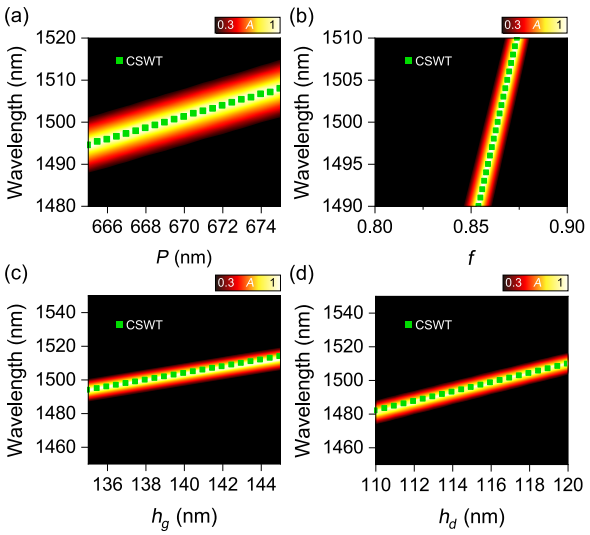

Fig. 4. The resonant absorption of graphene as a function of the resonant wavelength and (a) P, (b) f, (c) h_g, and (d) h_d are shown, respectively.

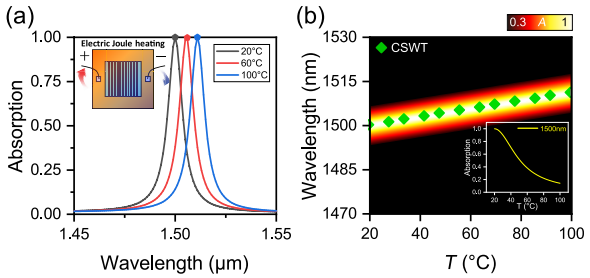

Fig. 5. (a) Absorption spectra at different T. (b) Absorption as a function of T and resonant wavelength.

in the system under various incident wavelengths. Different modes can be distinguished from the number of their nodes and absorption for GMR with higher-rank features more nodes and greater absorption. This may be ascribed to the spatial concentration of the electromagnetic energy. As shown in Fig. 3(e), GMR of third order traps more energy around graphene, resulting in higher consumption and greater absorption than other modes. Meanwhile, as h_g increases, resonant wavelength gradually red-shifts and manifests a linear dependence on h_g, as shown in Fig. 3(b) to Fig. 3(d). The absorption spectra and electrical maps when $h_g = 135$ nm are shown in Fig. 3(a) and Fig. 3(e). The theoretical values are calculated by CSWT once structural parameters are determined.

The absorption spectra as a function of the resonant wavelength and a variety of structural parameters are also investigated. It is demonstrated that grating period P, duty radio f which is defined as $f = W/P$, thickness of diffraction grating h_g, and dielectric layer h_d all characterize a linear relationship with the resonance wavelength, as shown in Fig. 4. The simulation results and theoretical values show more than just a significant agreement, in addition to a proportionality between the resonant wavelength and the structural parameters. This represented linear relationship can be greatly useful in the precise fabrication of optical devices. Intriguingly, the slope of the dotted line can be reasonably modified by changing the dielectric constant of materials and incident angle, according to CSWT.

The tunability of a fabricated device is significantly craving in the practical application all the way. The a-Si material is applied to our system to tackle the issue due to its linear and thermal adjustability. A variation of T is accountable for the change in the refractive index of a-Si, which causes a linear drift of the absorption peak. As shown in Fig. 5(a), the absorption peak redshifts the same wavelength as T increases from 20 °C to 100 °C. Importantly, the modification of T cannot impact the critical coupling since the absorption maintains a high level (above 99.7%) during the modulation process, which attributes the absorber a linear and nondestructive tunability. A top view of the system is shown in the inset to display electrically controlled Joule heating arrangement. [23] Figure 5(b) integrally demonstrates the absorption as a function of T and the incident wavelength and shows a linear dependence of resonant wavelength on T. In particular, the absorption decreases from 99.99% to 14.17% as T increases from 20 °C to 100 °C at a specific wavelength (1500nm), as shown in the inset.

Another remarkable tunable mechanism is that the absorption can be electrically controlled by modifying μ_c. As shown in Fig. 6(a), a layer of SiO_2 is introduced to electrically modulate μ_c by altering applied gate voltage. [24] The absorption spectrum of the new structure is demonstrated in Fig. 6(b), wherein the absorption peak somewhat redshifts (1500 nm to 1503 nm) compared with that in Fig. 2(a) with other impact factors keeping consistent. The dependence of absorption on

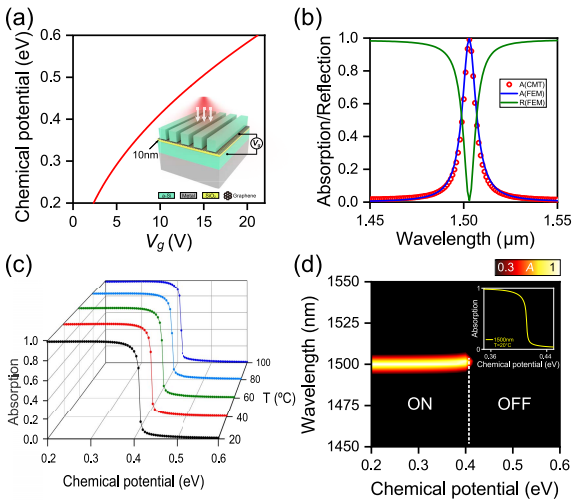

Fig. 6. (a) Dependency of μ_c on gate voltage. (b) Absorption and Reflection spectra from CMT and FEM results. (c) Absorption of graphene depends on μ_c at different T. (d) Absorption as a function of resonant wavelength and μ_c.

μ_c at different T is displayed in Fig. 6(c). It is indicated that all GMR mode absorption spectra experience a significant drop near 0.4 eV. More graphically, the absorption spectrum is apparently split into two sections, as shown in Fig. 6(d). The high absorption band exists in low μ_c ranges but dissipates greatly when μ_c is over 0.43 eV. Particularly, the absorptivity drops from 98.5% to 3.7% extremely with μ_c increasing from 0.35 eV to 0.45 eV when $T = 20$ °C at 1500 nm.

IV. Conclusion

We have demonstrated a GMR-type perfect absorber capable of thermal-electric tunability based on a-Si and graphene and investigated it in the NIR. The absorption enhancement is realized by critical coupling based on GMR, which can be illustrated by CMT and CSWT. It is numerically confirmed that a linear and nondestructive drift of absorption peak can be thermally achieved via electrically controlled Joule heating. Moreover, by means of modifying the applied gate voltage, one can realize a rapid switching of ON and OFF of the absorption. The proposed absorber may offer potential inspirations and applications in the area of graphene metamaterial as well as the optical absorber, modulator, and switching, etc.

References

[1] F. Bonaccorso, Z. Sun, T. Hasan, and A. C. Ferrari, "Graphene photonics and optoelectronics," *Nature Photon.*, vol. 4, no. 9, pp. 611–622, Sep. 2010.

[2] S. Luo, Y. Wang, X. Tong, and Z. Wang, "Graphene-based optical modulators," *Nanosc. Res. Lett.*, vol. 10, no. 1, p. 199, Dec. 2015.

[3] H.-J. Li, L.-L. Wang, J.-Q. Liu, Z.-R. Huang, B. Sun, and X. Zhai, "Investigation of the graphene based planar plasmonic filters," *Appl. Phys. Lett.*, vol. 103, no. 21, Nov. 2013, Art. no. 211104.

[4] Y. M. Qing, H. F. Ma, S. Yu, and T. J. Cui, "Ultra-narrowband absorption enhancement in monolayer transition-metal dichalcogenides with simple guided-mode resonance filters," *J. Appl. Phys.*, vol. 125, no. 21, Jun. 2019, Art. no. 213108.

[5] K. Wu, Y. Chen, J. Cheng, and K. Xu, "Use of carrier injection engineering to increase the light intensity of a polycrystalline silicon avalanche mode light-emitting device," *J. Appl. Phys.*, vol. 128, no. 17, Nov. 2020, Art. no. 173104.

[6] Y. M. Qing, H. F. Ma, Y. Z. Ren, S. Yu, and T. J. Cui, "Near-infrared absorption-induced switching effect via guided mode resonances in a graphene-based metamaterial," *Opt. Exp.*, vol. 27, no. 4, pp. 5253–5263, 2019.

[7] Y. M. Qing, Y. Ren, D. Lei, H. F. Ma, and T. J. Cui, "Strong coupling in two-dimensional materials-based nanostructures: A review," *J. Opt.*, vol. 24, no. 2, Feb. 2022, Art. no. 024009.

[8] D. Jariwala, T. J. Marks, and M. C. Hersam, "Mixed-dimensional van der Waals heterostructures," *Nature Mater.*, vol. 16, no. 2, pp. 170–181, Feb. 2017.

[9] A. N. Grigorenko, M. Polini, and K. S. Novoselov, "Graphene plasmonics," *Nature Photon.*, vol. 6, no. 11, pp. 749–758, Nov. 2012.

[10] J. R. Piper and S. Fan, "Total absorption in a graphene monolayer in the optical regime by critical coupling with a photonic crystal guided resonance," *ACS Photon.*, vol. 1, no. 4, pp. 347–353, 2014.

[11] J.-H. Hu et al., "Enhanced absorption of graphene strips with a multilayer subwavelength grating structure," *Appl. Phys. Lett.*, vol. 105, no. 22, 2014, Art. no. 221113.

[12] J. Tian, Q. Li, J. Lu, and M. Qiu, "Reconfigurable all-dielectric antenna-based metasurface driven by multipolar resonances," *Opt. Exp.*, vol. 26, no. 18, pp. 23918–23925, 2018.

[13] A. Thomas, P. Savaliya, K. Kumar, A. Ninawe, and A. Dhawan, "Au nanowire-VO_2 spacer-Au film based optical switches," *J. Opt. Soc. Amer. B, Opt. Phys.*, vol. 35, no. 7, pp. 1687–1697, 2018.

[14] Q.-Y. Wen et al., "A tunable hybrid metamaterial absorber based on vanadium oxide films," *J. Phys. D, Appl. Phys.*, vol. 45, no. 23, Jun. 2012, Art. no. 235106.

[15] H. Liu, Z.-H. Wang, L. Li, Y.-X. Fan, and Z.-Y. Tao, "Vanadium dioxide-assisted broadband tunable terahertz metamaterial absorber," *Sci. Rep.*, vol. 9, no. 1, p. 5751, Dec. 2019.

[16] M. J. Dicken et al., "Frequency tunable near-infrared metamaterials based on VO_2 phase transition," *Opt. Exp.*, vol. 17, no. 20, pp. 18330–18339, 2009.

[17] D. Hohlfeld and H. Zappe, "An all-dielectric tunable optical filter based on the thermo-optic effect," *J. Opt. A, Pure Appl. Opt.*, vol. 6, no. 6, pp. 504–511, Jun. 2004.

[18] H. Lu, X. Gan, D. Mao, Y. Fan, D. Yang, and J. Zhao, "Nearly perfect absorption of light in monolayer molybdenum disulfide supported by multilayer structures," *Opt. Exp.*, vol. 25, no. 18, pp. 21630–21636, 2017.

[19] G. W. Hanson, "Dyadic Green's functions and guided surface waves for a surface conductivity model of graphene," *J. Appl. Phys.*, vol. 103, no. 6, 2008, Art. no. 064302.

[20] S. Fan, W. Suh, and J. D. Joannopoulos, "Temporal coupled-mode theory for the Fano resonance in optical resonators," *J. Opt. Soc. Amer. A, Opt. Image Sci.*, vol. 20, no. 3, pp. 569–572, Mar. 2003.

[21] S. S. Wang and R. Magnusson, "Multilayer waveguide-grating filters," *Appl. Opt.*, vol. 34, no. 14, pp. 2414–2420, May 1995.

[22] K. Xu, "Silicon electro-optic micro-modulator fabricated in standard CMOS technology as components for all silicon monolithic integrated optoelectronic systems," *J. Micromech. Microeng.*, vol. 31, no. 5, May 2021, Art. no. 054001.

[23] M. J. Uddin and R. Magnusson, "Guided-mode resonant thermo-optic tunable filters," *IEEE Photon. Technol. Lett.*, vol. 25, no. 15, pp. 1412–1415, Aug. 1, 2013.

[24] Y. M. Qing, H. F. Ma, and T. J. Cui, "Theoretical analysis of tunable multimode coupling in a grating-assisted double-layer graphene plasmonic system," *ACS Photon.*, vol. 6, no. 11, pp. 2884–2893, Nov. 2019.